Chemical Engineering Science 152 (2016) 579–585

Contents lists available at ScienceDirect

Chemical Engineering Science

journal homepage: www.elsevier.com/locate/ces

An analytical relation for the void fraction distribution in a fully developed bubbly flow in a vertical pipe

O. Marfaing [a,*], M. Guingo [b], J. Laviéville [b], G. Bois [a], N. Méchitoua [b], N. Mérigoux [b], S. Mimouni [b]

[a] Den-Service de Thermo-hydraulique et de Mécanique des Fluides (STMF), CEA, Université Paris-Saclay, F-91191, Gif-sur-Yvette, France
[b] Electricité de France R&D Division, 6 Quai Watier, F-78400 Chatou, France

HIGHLIGHTS

- We perform an analytical study of an upward bubbly flow in a pipe.
- Drag, dispersion, lift, and wall forces are considered with constant coefficients.
- The void fraction profile is expressed analytically as a function of the liquid velocity and pressure.
- The relation is valid for high Reynolds number flows.
- At the wall, the void fraction is zero, due to the singular wall force.
- Numerical calculations are performed with a CFD code.

ARTICLE INFO

Article history:
Received 8 April 2016
Received in revised form
15 June 2016
Accepted 17 June 2016
Available online 18 June 2016

Keywords:
Two-fluid model
Analytical relation
Verification
Wall force
Lift force
Dispersion force
Drag force
NEPTUNE_CFD

ABSTRACT

The problem of a steady, axisymmetric, fully developed adiabatic bubbly flow in a vertical pipe is studied analytically with the two-fluid model. The exchange of momentum between the phases is described as the sum of drag, lift, wall and dispersion contributions, with constant coefficients.

Under these conditions, we are able to express analytically the void fraction profile as a function of the liquid velocity and pressure profiles. This relation is valid independently of the Reynolds stress model in the liquid phase – and can serve as a verification case for multiphase flow codes.

The analytical void fraction profile vanishes at the wall, as a result of the balance between dispersion and wall forces. It presents a peak near the wall for upward flows, whereas its maximum is reached in the center of the pipe for downward flows. This is illustrated by calculations performed for upward and downward bubbly flows with the NEPTUNE_CFD code.

1. Introduction

Two-phase (or multiphase) flows are encountered in many industrial situations related to nuclear or chemical engineering. In order to address the growing need for simulations, the models and numerical schemes used in industrial codes need to be properly verified and validated (Podowski, 2014; Boyd, 2014).

Two-phase flows are characterized by the presence of (numerous) interfaces which separate local single-phase regions. The microscopic (or DNS) description of such a flow requires to solve the local instantaneous Navier–Stokes equations for each phase and to locate interface positions at every time. Because of its prohibitive cost, this approach is rarely used in practice. Instead, the knowledge of averaged quantities is often sufficient for applications. For these reasons, macroscopic approaches have been developed.

The two-fluid model (Morel, 2015; Ishii and Hibiki, 2010; Drew and Passman, 1999; Ishii and Kocamustafaogullari, 1983) belongs to these macroscopic descriptions of two-phase flows. It can be mathematically derived by averaging the local instantaneous equations. Every physical quantity is therefore decomposed into its average and fluctuations. Through the averaging procedure, the details of the microscopic formulation are partially eliminated. However, these small structures still influence the overall flow and therefore need to be accounted for by proper closure relations. Developing proper closure relations which are valid over a wide

* Corresponding author.
E-mail address: olivier.marfaing@cea.fr (O. Marfaing).

http://dx.doi.org/10.1016/j.ces.2016.06.041
0009-2509/

Notations

B	constant in Eq. (22), determined from the knowledge of the average void fraction over a cross-section
C_D	drag coefficient
C_L	lift coefficient
C_{W1},C_{W2}	wall coefficients
d_b	bubble diameter (m)
D_{eff}	effective dispersion coefficient (m^2/s)
D_{eff^*}	non-dimensional effective dispersion coefficient
g	gravity (m^2/s)
M_g	interfacial momentum exchange term (Pa/m)
r	radial coordinate (m)
r^*	non dimensional radial coordinate defined by (14)
R	radius of the pipe (m)
R^*	non dimensional radius of the pipe defined by (14)
U_R	relative velocity (m/s)
V_k	velocity of phase k (m/s)
y	distance to the wall (m)
y^*	non-dimensional distance to the wall
Y^*	non-dimensional quantity defined by (21)
z	axial coordinate (m)

Greek letters

α_k	volume fraction of phase k
μ_k	viscosity of phase k
ρ_k	density of phase k

Subscripts

k	k-th phase
g	gas phase
l	liquid phase

Mathematical operators

$sgn(x)$	sign of x: equals 1 for $x>0$ and -1 for $x<0$.

range of flow conditions – e.g. for momentum transfer between the phases – is still today a challenging task. Experimental data and DNS simulations are two important ways to complete it. Although analytical approaches are comparatively rare in this area, we believe they can contribute to this effort, by providing insight on the mathematical properties of models.

One of the difficulties in the verification of two-fluid (or multiphase) flow solvers is the coupling between phases, which makes the search for analytical solutions more difficult, when compared to single-phase flows. In the two-fluid formalism, a balance equation is written for the mass and momentum of each phase, and the coupling between the liquid and the gas is accounted for by an interfacial exchange term in the momentum balances.

In this paper, we consider the problem of a (statistically) steady, axisymmetric, fully developed adiabatic bubbly flow in a vertical pipe – here, "statistically" means that only the average flow (not its fluctuations) is steady, axisymmetric and fully developed, see e.g. [5, §2.2]. In order to perform an analytical study, simplifying assumptions are introduced:

(i) the average flow is steady, axisymmetric and fully developed. Variations in the gas and liquid densities are therefore neglected.

(ii) all bubbles have the same diameter, denoted by d_b.

(iii) the interfacial exchange term is the sum of four contributions: drag, lift, wall, and dispersion forces. The expressions of these forces (see Section 2) are assumed to have constant coefficients. Note that virtual mass effects do not play a role in a developed steady flow.

(iv) viscous and Reynolds stresses are neglected in the gas phase momentum equation (see discussion in Section 2).

The physical significance of these assumptions is discussed in Section 2.

Under these conditions, we are able to give an analytical expression for the void fraction profile, as a function of the liquid velocity and pressure profiles. The derivation of this analytical expression requires no specific assumption on Reynolds stresses in the liquid phase. Of course, the velocity and pressure profiles still need to be calculated by a numerical solver. In the same time, in view of this generality, this analytical expression can serve as a verification case for multiphase flow codes.

The void fraction profile has a peak near the wall for upward flows, whereas core-peaking is observed for downward flows. We also show that the compensation between wall and dispersion forces causes the void fraction to vanish at the wall.

In Section 4, calculations are performed for upward and downward bubbly flows with the NEPTUNE_CFD code (Guelfi et al., 2007; Guingo et al., 3–6 May 2015). NEPTUNE_CFD is a Computational Multi-Fluid Dynamics code dedicated to the simulation of multiphase flows, primarily targeting nuclear thermal-hydraulics applications, such as the departure from nuclear boiling (DNB) or the two-phase Pressurized Thermal Shock (PTS). It has been developed within the joint NEPTUNE R&D project (AREVA, CEA, EDF, IRSN) since 2001.

2. Presentation of the problem

In this work, we make use of the two-fluid model (Morel, 2015; Ishii and Hibiki, 2010; Drew and Passman, 1999) to describe a bubbly flow in a vertical pipe. We consider an adiabatic bubbly flow in a vertical cylindrical pipe with radius R (see Fig. 1). The flow is assumed to be statistically steady, axisymmetric, and fully developed – here, "statistically" means that only the average flow (not its fluctuations) is steady, axisymmetric and fully developed, see e.g. [5, §2.2]. In particular, no phase change occurs, and the variations in the gas and liquid densities are neglected.

In all what follows, we denote with subscript g (resp. l)

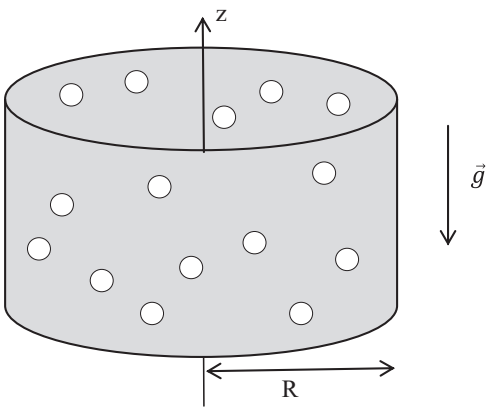

Fig. 1. Bubbly flow in a vertical pipe.

quantities relating to the gas (resp. liquid) phase. For $k = g$ or l, the mass balance for phase k writes:

$$\frac{\partial}{\partial t}(\alpha_k\rho_k)+\nabla.\left(\alpha_k\rho_k\vec{V}_k\right)=0 \tag{1}$$

Because the flow is steady and fully developed, it follows that the radial component of velocity $\vec{V}_k$ is nil, while its axial component only depends on r. So we can write:

$$\vec{V}_k = V_k(r)\vec{e}_z \tag{2}$$

Now we come to the momentum balance. For the derivation of our analytical relation, the momentum balance is written only for the gas phase, in the radial and axial directions. In particular it means we need no specific assumption on the Reynolds stress tensor in the liquid phase.

Viscous and Reynolds stresses are neglected in the gas phase momentum balance, an assumption that is widely used in theoretical studies of low Reynolds number (or "laminar") bubbly flows (Azpitarte and Buscaglia, 2003; Antal et al., 1991). This simplification is sometimes used for turbulent flows, but its validity is then questionable: indeed, for such flows, the turbulence in the liquid phase will drive Reynolds stresses in the gas phase – see for instance (Morel, 2015; Chap 10) or (Laviéville et al., September 2015, Section 2.2.3) and references therein. So, from a physical viewpoint, our models are more appropriate for laminar bubbly flows. Nevertheless, because the derivation involves no assumption on liquid Reynolds stresses, our analytical solution can also be used as a verification tool for CFD simulations of high Reynolds number flows, provided the CFD code also neglects gas Reynolds stresses.

The momentum balance for the gas phase can then be written:

$$\frac{\partial}{\partial t}\left(\alpha_g\rho_g\vec{V}_g\right)+\nabla.\left(\alpha_g\rho_g\vec{V}_g\vec{V}_g\right)=-\alpha_g\nabla\vec{P}+\alpha_g\rho_g\vec{g}+\vec{M}_g \tag{3}$$

In the above equation, $\vec{M}_g$ stands for the interfacial momentum exchange term. The modeling of this term is now discussed. Then, in Section 3, we write the axial and radial components of Eq. (3) and derive the analytical relation between the void fraction and the liquid velocity and pressure profiles.

As explained in the introduction, the interfacial momentum transfer term $\vec{M}_g$ is written as the sum of four contributions: drag, lift, wall, and dispersion force, all of which have constant coefficients.

Because of Eq. (2), it can be seen that material derivatives of the form $\frac{\partial}{\partial t}\vec{V}_k+\left(\vec{V}_k.\nabla\right)\left(\vec{V}_k\right)$ cancel, so the contribution of virtual mass is nil.

In the following, we denote by

$$\vec{U}_R \equiv \vec{V}_g - \vec{V}_l \tag{4}$$

the relative velocity between the phases.

2.1. The drag force

The contribution of the drag force is expressed in the following way:

$$\vec{M}_g^{\,D} = -\frac{3}{4}\alpha_g\rho_l\frac{C_D}{d_b}\left|\vec{U}_R\right|\vec{U}_R \tag{5}$$

where d_b stands for the (constant) bubble diameter, and C_D is the drag coefficient, which is here assumed to be constant.

2.2. The dispersion force

The dispersion force, proportional to the void fraction gradient, results in the migration of bubbles from high to low void fraction regions. This effect is interpreted as the fluctuating part of other forces, in the averaging process leading to the two-fluid model (Morel, 2015, Chp. 7).

Several models have been developed (Davidson, 1990; Lopez de Bertodano, 1998; Burns et al., 2004; Krepper et al., Prasser; Laviéville et al., September 2015; Lopez de Bertodano, 1998; Gosman et al., 1992) in the literature to take into account this diffusive effect. In (Davidson, 1990), Davidson expresses it as the product of the drag function and an apparent mean drift velocity of the liquid relative to the gas phase: $\vec{M}_g^{\,disp} = -\frac{3}{4}\alpha_l\rho_l\frac{C_D}{d_b}\left|\vec{U}_R\right|D_{\text{eff}}\nabla\vec{\alpha}_g$ where D_{eff} is an effective bubble dispersion coefficient, considered as constant.

The model proposed by Gosman et al., (1992) uses the liquid turbulent viscosity μ_l^T. It writes: $\vec{M}_g^{\,disp} = -\frac{3}{4}\frac{C_D}{\alpha_l^2 d_b}\mu_l^T\left|\vec{U}_R\right|\nabla\vec{\alpha}_g$. A similar approach is followed by Krepper et al..

In Lopez de Bertodano (1998), Lopez de Bertodano expresses the transfer term as a function of the liquid turbulent kinetic energy $\vec{M}_g^{\,disp} = -\rho_l k_l\frac{1}{St(1+St)}\nabla\vec{\alpha}_g$ where the Stokes number St is defined as the ratio of the relaxation times of the bubbles and the eddies. In Laviéville et al. (September 2015) introduce a similar form.

In this work we will adopt the following model, very close to Davidson's expression.

$$\vec{M}_g^{\,disp} = -\frac{3}{4}\rho_l\frac{C_D}{d_b}\left|\vec{U}_R\right|D_{\text{eff}}\nabla\vec{\alpha}_g \tag{6}$$

where we simply removed the dependence upon the liquid volume fraction (which can be assumed to be approximately 1 in the case of low void fraction). Again, the bubble dispersion coefficient D_{eff} is assumed to be constant.

2.3. The lift force

The contribution of the lift force is expressed in the following way:

$$\vec{M}_g^{\,L} = -\alpha_g\rho_l C_L\vec{U}_R\times\left(\vec{\text{rot}}\vec{V}_l\right) \tag{7}$$

where the lift coefficient C_L is here assumed to be constant.

2.4. The wall force

The wall force is close to Antal's et al. (1991) model:

$$\vec{M}_g^{\,W} = 2\alpha_g\rho_l\frac{\left|U_{R,\parallel}\right|^2}{d_b}\text{Max}\left[0, C_{W1}+C_{W2}\frac{d_b}{2y}\right]\vec{n}_W \tag{8}$$

where $C_{W1} = -0.1$ and $C_{W2} = 0.147$ are taken as constants, y stands for the distance to the wall, and $U_{R,\parallel}$ denotes the component of the relative velocity parallel to the wall.

With this expression, the bubbles are pushed away from the wall if they are at a distance $y < -\frac{C_{W2}}{2C_{W1}}d_b$. The Max function guarantees that they are not attracted if $y > -\frac{C_{W2}}{2C_{W1}}d_b$.

Before deriving the analytical relation in the next section, let us discuss our constant-coefficient assumptions.

In many bubbly flow simulations, correlations are used to express the drag coefficient C_D as a function of the particle Reynolds number $Re_b = \rho_l U_R d_b / \mu_l$. For instance Ishii and Zuber, (1979) propose the following relation $C_D = \frac{24}{Re_b}(1 + 0.1Re_b^{3/4})$. For bubble Reynolds numbers larger than 200, the second term is seen to vary as $Re_b^{-1/4}$. So, clearly, assuming a constant drag coefficient is an approximation, but we can say that correlations predict a slow variation of the drag coefficient with the bubble Reynolds number.

An empirical correlation was proposed by Tomiyama (June 1998) for the lift force. The lift coefficient is expressed as a function of the bubble Reynolds number and the (modified) Eötvös number, based on the maximum horizontal dimension of bubbles, and which can, in turn, be estimated as a function of the Eötvös number through Wellek's correlation (Wellek et al., 1966). Again, for bubble Reynolds numbers larger than 200, C_L varies slowly with Re_b, and Eötvös number is known as soon as the bubble diameter is known.

Furthermore, it must be mentioned that if the drag coefficient is assumed to be only a function of the bubble Reynolds number, as in Ishii and Zuber's correlation, and the lift coefficient is assumed to depend only on the bubble Reynolds number and the Eötvös number, the analytical solution derived in Section 3 is still valid, since the relative velocity U_R, and therefore the drag and lift coefficients, are uniform (see Eq. (10) in the next section).

In the wall force model developed by Antal et al. (1991), C_{W2} is a constant with value -0.147 whereas C_{W1} has the form $C_{W1}= -0.104 - 0.06\,|U_R|$ (with U_R in m/s). So when U_R is in the range 0-1 m/s, the variations of C_{W1} are not negligible, but again, with a uniform relative velocity, the coefficient is uniform and the calculations of Section 3 are still valid. Simulations performed in the literature often consider both C_{W1} and C_{W2} as constant, sometimes with other values.

Finally, the dispersion model with constant coefficient was used by Davidson to compute a bottom gas injection in a liquid pool (Castillejos and Brimacombe, 1986). The coefficient D_{eff} is chosen as (a global value of) the liquid turbulent kinematic viscosity.

3. The analytical relation

3.1. Momentum balance for the gas phase in the axial and radial directions

Using Eqs. (2), (4), (5)–(8), the gas phase momentum balance (3) is now projected in axisymmetric cylindrical coordinates.

From Eq. (2), the left hand side of the momentum balance, that is, quantity $\frac{\partial}{\partial t}\left(\alpha_g\rho_g\vec{V_g}\right) + \nabla.\left(\alpha_g\rho_g\vec{V_g}\vec{V_g}\right)$, is zero.

3.2. Axial direction

The flow being steady and fully-developed, the axial momentum equation reduces to:

$$0 = -\alpha_g\rho_g g - \alpha_g\frac{\partial P}{\partial z} - \frac{3}{4}\alpha_g\rho_l\frac{C_D}{d_b}|U_R|U_R \tag{9}$$

Simplifying by the void fraction, it follows that the relative velocity is constant and uniform in the pipe, with value given by:

$$|U_R|U_R = -\frac{4d_b}{3\rho_l C_D}\left(\rho_g g + \frac{\partial P}{\partial z}\right) \tag{10}$$

We recall that, for a fully developed flow, the axial pressure gradient $\frac{\partial P}{\partial z}$ is independent of r.

For bubbly flows, the main phase is the liquid. So the axial pressure gradient is of the order of magnitude of the hydrostatic pressure gradient for a liquid column:

$$\frac{\partial P}{\partial z} \sim -\rho_l g. \tag{11}$$

Because the liquid density is much larger than the gas density, Eqs. (10) and (11) imply that the relative velocity U_R is positive.

At this point a small digression: we insist that Eq. (11) does not necessarily mean that the fluid velocity is *small*. To illustrate this, consider a single-phase flow in a vertical tube: the pressure gradient is the sum of the hydrostatic pressure gradient and the pressure loss due to wall friction. The latter can be expressed as $\left(\partial P/\partial z\right)_{\text{friction}} = f\rho_l\bar{U}^2/4R$ with f the friction factor (Pope, 2000, Section 7.2). So $\frac{\partial P}{\partial z} \sim -\rho_l g$ means that the Froude number $Fr=\bar{U}^2/2gR$ is smaller than $1/f$. For a smooth pipe with radius $R=19$ mm as in the calculations of Section 4, it means that the average velocity $\bar{U}$ is smaller than 3 m/s.

3.3. Radial direction

The projection of Eq. (3) onto the radial direction writes:

$$0 = -\alpha_g\frac{\partial P}{\partial r} - \alpha_g C_l\rho_l U_R\frac{\partial V_l}{\partial r} - 2\alpha_g\rho_l\frac{|U_R|^2}{d_b}F_W - \frac{3}{4}\rho_l\frac{C_D}{d_b}|U_R|D_{\text{eff}}\frac{\partial\alpha_g}{\partial r} \tag{12}$$

where we have set:

$$F_W = \text{Max}\left[0, C_{W1} + C_{W2}\frac{d_b}{2(R-r)}\right] \tag{13}$$

Rearranging terms in (12), and simplifying by the void fraction, it follows:

$$\frac{1}{\alpha_g}\frac{\partial\alpha_g}{\partial r} = -\frac{4}{3}\frac{d_b}{C_D\rho_l|U_R|D_{\text{eff}}}\frac{\partial P}{\partial r} - \frac{4}{3}\frac{C_L d_b}{C_D D_{\text{eff}}}\frac{\partial V_l}{\partial r} - \frac{8}{3}\frac{|U_R|}{C_D D_{\text{eff}}}F_W \tag{14}$$

From Eq. (10), U_R is a constant, and Eq. (14) can then be integrated analytically.

We begin by rewriting Eq. (14) in non-dimensional form. As in Eq. (8), $y = R - r$ denotes the distance to the wall. Let

$$y^* \equiv \frac{2y}{d_b},\ r^* \equiv \frac{2r}{d_b},\ R^* \equiv \frac{2R}{d_b} \tag{15}$$

be the non-dimensional spatial coordinates,

$$V_l^* \equiv \frac{V_l}{|U_R|},\quad P^* \equiv \frac{P}{\rho_l|U_R|^2} \tag{16}$$

be the non-dimensional liquid velocity and the non-dimensional pressure, and

$${D_{\text{eff}}}^* \equiv \frac{3}{4}\frac{C_D D_{\text{eff}}}{|U_R|d_b} \tag{17}$$

be the non-dimensional bubble dispersion coefficient.

(14) can be rewritten:

$$\frac{1}{\alpha_g}\frac{\partial\alpha_g}{\partial y^*} = -\frac{1}{{D_{\text{eff}}}^*}\frac{\partial P^*}{\partial y^*} - \frac{C_L}{{D_{\text{eff}}}^*}\frac{\partial V_l^*}{\partial y^*} + \frac{F_W}{{D_{\text{eff}}}^*} \tag{18}$$

$$F_W = \text{Max}\left[0, C_{W1} + \frac{C_{W2}}{y^*}\right].$$

On the domain $0 < y^* < -\frac{C_{W2}}{C_{W1}}$, Eq. (18) writes:

$$\frac{1}{\alpha_g}\frac{\partial\alpha_g}{\partial y^*} = -\frac{1}{{D_{\text{eff}}}^*}\frac{\partial P^*}{\partial y^*} - \frac{C_L}{{D_{\text{eff}}}^*}\frac{\partial V_l^*}{\partial y^*} + \frac{1}{{D_{\text{eff}}}^*}\left(C_{W1} + \frac{C_{W2}}{y^*}\right) \tag{19}$$

and integrates into.

$$\alpha_g = B \times \left(y^*\right)^{C_{W2}/{D_{\text{eff}}}^*}\exp\left(\frac{C_{W1}}{{D_{\text{eff}}}^*}y^*\right)\exp\left(-\frac{C_L}{{D_{\text{eff}}}^*}V_l^*\right)\exp\left(-\frac{P^* - P^*|_{y=0}}{{D_{\text{eff}}}^*}\right) \tag{20}$$

where B is a constant. In the last factor, $P^*|_{y=0} = P^*|_{r=R}$ is the pressure at the wall. Because the flow is developed, the pressure

difference $P^* - P^*|_{r=R}$ is independent of the axial coordinate z. So the use of the pressure difference in the last factor of (20), instead of pressure P^*, ensures that B is independent of z as well.

Similarly, for $y^* > -\frac{C_{W2}}{C_{W1}}$, we have.

$$\alpha_g = B' \exp\left(-\frac{C_L}{D_{\text{eff}}^*} V_l^*\right) \exp\left(-\frac{P^* - P^*|_{r=R}}{D_{\text{eff}}^*}\right) \tag{21}$$

where B' is another constant.

Expressions (20) and (21) have to connect continuously at $y^* = -\frac{C_{W2}}{C_{W1}}$. So let Y^* be defined by:

$$Y^* \equiv \min\left(-\frac{C_{W2}}{C_{W1}}; y^*\right) = \min\left(-\frac{C_{W2}}{C_{W1}}; R^* - r^*\right) \tag{22}$$

The following expression is now valid on the whole domain:

$$\alpha_g = B \times \left(Y^*\right)^{C_{W2}/D_{\text{eff}}^*} \exp\left(\frac{C_{W1}}{D_{\text{eff}}^*} Y^*\right) \exp\left(-\frac{C_L}{D_{\text{eff}}^*} V_l^*\right) \exp\left(-\frac{P^* - P^*|_{r=R}}{D_{\text{eff}}^*}\right) \tag{23}$$

with B a constant, which can be determined, knowing for instance the void fraction at the center of the pipe, or the integral void fraction.

3.3. Discussion

Eq. (23) shows that the void fraction profile results from an equilibrium between lift, wall and dispersion forces.

The effect of the lift force, expressed in the factor $\exp\left(-\frac{C_L}{D_{\text{eff}}^*} V_l^*\right)$, is seen to depend on the sign of the liquid velocity and the lift coefficient. Assume the latter is positive. For upward flows, V_l^* is maximum at the center of the pipe, and minimum at the wall. So the bubbles are pushed towards the wall. On the opposite, in downward flows, V_l^* is negative, and the bubbles accumulate in the central region of the pipe, where the liquid velocity is minimum.

Due to the wall force, the void fraction is zero at the wall. Coming back to Eq. (19), we can thus see that, when the distance to the wall y tends to zero, the dominant terms in the radial momentum equation are dispersion and wall forces, which counterbalance each other. This can be seen from Eq. (14), after simplification by the void fraction: because the diffusion coefficient D_{eff} does not vanish at the wall, the wall force term F_W, which goes to infinity when y^* tends to zero, can be "absorbed" by the term proportional to $\frac{D_{\text{eff}}}{\alpha_g}\frac{\partial \alpha_g}{\partial r}$. Note that this counterbalancing between dispersion and wall force can still take place if coefficient D_{eff} vanishes at the wall, for instance if D_{eff} decreases more slowly than α_g(eg as ${\alpha_g}^s$ with parameter $s < 1$). This possibility does not seem to have been widely explored yet. Many models of dispersion force from the literature are derived in regions far away from the walls, where some gradients (of velocity or velocity covariance) can be neglected. We believe the derivation of dispersion models specific to near-wall regions would be an important topic of investigation.

In the next section, the discussion is illustrated by calculations performed with the NEPTUNE_CFD code.

4. Numerical calculations

The problem being axisymmetric, the computational domain is limited to a sector of cylinder with an opening angle of 10°. The radius R of the pipe is set to 19 mm. The meshes used are uniform in the radial direction, with one cell both in the axial and orthoradial directions. Symmetry boundary conditions are imposed on the azimuthal planes.

In order to compute a developed solution, periodic boundary conditions are imposed on the top and bottom sections of the pipe. The pressure gradient is imposed as a volumetric source term. In order to compute a steady solution, calculations are run with the transient solver of NEPTUNE_CFD until the void fraction profile is seen to be steady. In most cases, the void fraction profiles reach a steady state after 15 s, and the calculations are stopped at 20 s.

The liquid (resp. gas) density is set to 1000 kg/m^3 (resp. 1 kg/m^3). The liquid (resp. gas) dynamic viscosity is set to 10^{-3} kg m^{-1} s^{-1} (resp. 10^{-5} kg m^{-1} s^{-1}). The bubble diameter is 2.5 mm. The drag, lift and non-dimensional dispersion coefficients are taken as $C_D = 0.1$, $C_L = 0.03$ and $D_{eff}^* = 0.003$.

As in the theoretical analysis of Sections 2 and 3, the simulations neglect Reynolds stresses in the gas phase momentum balance. As discussed in Section 2, from a physical viewpoint, this assumption is more adapted to low Reynolds number bubbly flows (Azpitarte and Buscaglia, 2003; Antal et al., 1991). Nevertheless, because the analytical work of Section 3 involves no assumption on liquid Reynolds stresses, our analytical solution can also be used as a verification tool for CFD simulations of high Reynolds number flows.

Because at present NEPTUNE_CFD is dedicated to the simulation of turbulent flows, the calculations of Sections 4.1 and 4.2 are run for Reynolds numbers of the order of 20 000. Turbulence in the liquid phase is accounted for with a k–ε model.

In all cases below, the theoretical profile given by relation (23) is computed with the numerical velocity and pressure fields calculated by the solver. As explained in the end of Section 3.1, the factor B in (23) is determined by the numerical value of the void fraction at radial position $r = 0$.

4.1. Upward bubbly flow

At initial time, t = 0 s, the void fraction is uniform with value 0.02. In this calculation, the imposed pressure gradient $\partial P/\partial z$ is set to -9712 Pa m^{-1}, slightly below the hydrostatic pressure gradient $-\alpha_g \rho_g g - \alpha_l \rho_l g$.

Two meshes were used, respectively with 500 and 1000 cells in the radial direction.

The void fraction profiles are displayed in Fig. 2. The dashed lines correspond to the calculations on both meshes, while the solid line is the analytical profile given by application of Eq. (23).

The 500-cell and 1000-cell calculations are seen to be close to each other, while the analytical profile is almost superposed with the 1000-cell result.

The analytical and numerical curves are seen to be close to each other. As discussed in Section 3.4, in this upward bubbly flow configuration, bubbles accumulate in the near-wall region: the void fraction profile is seen to be almost uniform in the center of the pipe, to reach a maximum at a distance of the order of one bubble radius from the wall, and then to decrease at the wall.

The liquid velocity profile is displayed in Fig. 3. The flow we considered is turbulent, with a Reynolds number of order 20,000.

Fig. 4 presents a more detailed view of the void fraction profile in the near-wall region. Computations with four different grid refinements are displayed. For the two coarsest grids, respectively 50 or 100 cells, the computed profiles are seen to be too spread. The peak begins to be well computed from 500 cells, that is, a mesh size of about 1/50 of the bubble diameter.

Many CFD studies of bubbly flows in pipes do not use grids with cells significantly smaller than the bubble size. Liu and Bankoff's experiments (Liu and Bankoff, 1993) – where the test section has the same diameter as in our numerical case – are often calculated with 50 or 100 cells in the radial direction. This example emphasizes the need for refined calculations, that is calculations with mesh sizes significantly lower than the bubble diameter.

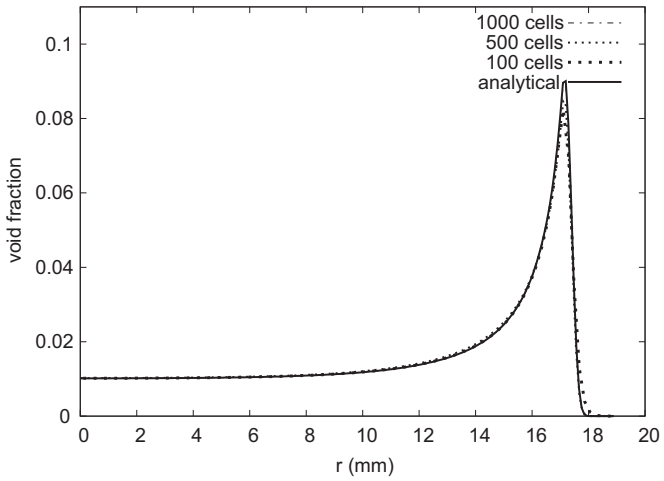

Fig. 2. Void fraction profile for an upward flow with C_D =0.1, D_{eff}^* =0.003, C_L=0.03, C_{W1}=−0.1, C_{W2} =0.147.

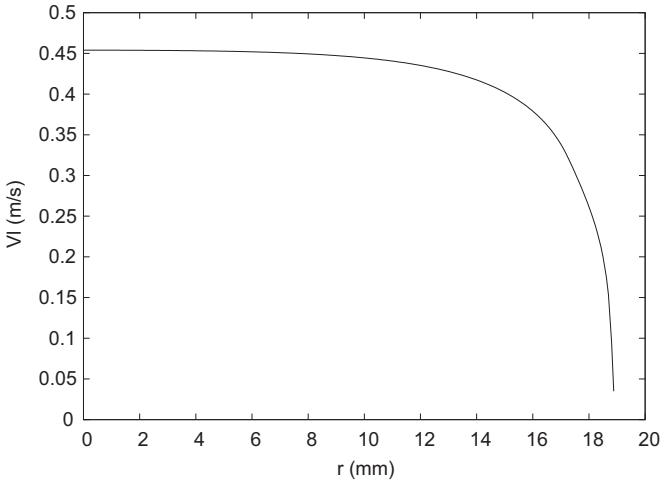

Fig. 3. Liquid velocity profile for an upward flow with C_D=0.1, D_{eff}^* =0.003, C_L =0.03, C_{W1}=−0.1, C_{W2}=0.147.

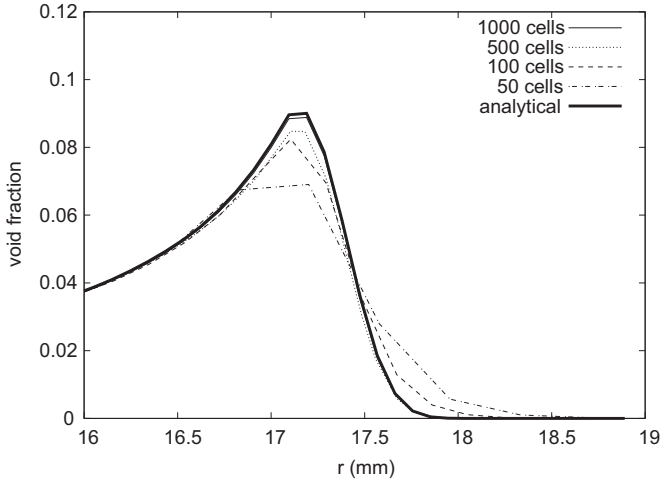

Fig. 4. Void fraction profile for an upward flow with C_D=0.1, D_{eff}^* =0.003, C_L=0.03, C_{W1}=−0.1, C_{W2}=0.147 – zoom on the near-wall region.

4.2. Downward bubbly flow

At initial time, t=0, the void fraction field is uniform with value 0.02. The pressure gradient $\partial P/\partial z$ is now set to $-9515\ \mathrm{Pa\ m^{-1}}$,

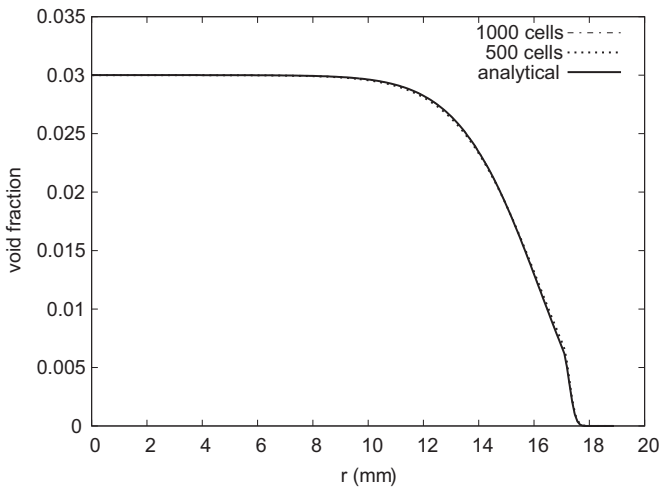

Fig. 5. Void fraction profile for the downward bubbly flow with C_D =0.1, D_{eff}^* = 0.003, C_L =0.03, C_{W1}=−0.1, C_{W2} =0.147.

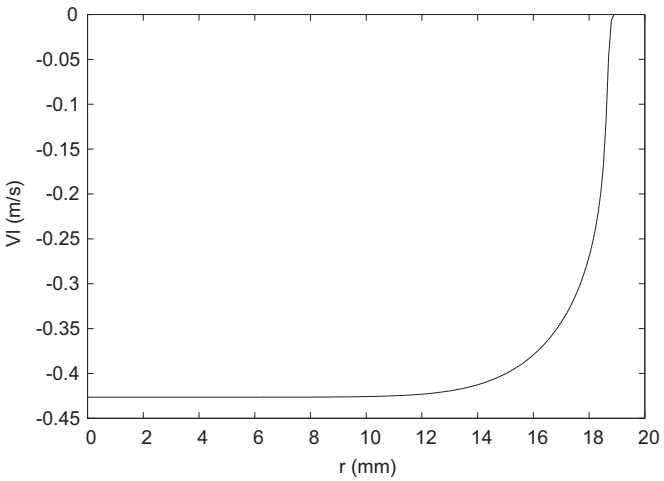

Fig. 6. Liquid velocity profile for the downward bubbly flow with C_D = 0.1, D_{eff}^* = 0.003, C_L =0.03, C_{W1}=−0.1, C_{W2} = 0.147.

slightly above the hydrostatic pressure gradient $-\alpha_g\rho_g g-\alpha_l\rho_l g$. The drag, dispersion, lift and wall coefficients are taken as before as C_D=0.1, D_{eff}^* = 0.003, C_L =0.03, C_{W1}=-0.1, C_{W2}=0.147.

In Fig. 5, we display the analytical void fraction profile and the numerical profile obtained in the 500 and 1000-cell calculations.

The analytical and numerical curves are seen to be almost superposed. Unlike the upward bubbly flow case, the void fraction reaches its maximum at the center of the pipe, where the profile is almost flat. Fig. 6 shows the liquid velocity profile. Again, the Reynolds number is about 20,000.

5. Conclusion

In this work, we perform an analytical study of the problem of a statistically steady axisymmetric fully developed adiabatic bubbly flow in a vertical pipe. The analysis is conducted with the two-fluid formalism.

The interfacial momentum transfer $\vec{M}_g$ is modeled as the sum of four contributions: drag, dispersion, lift, and wall forces, with constant coefficients. Note that the virtual mass effects do not play a role in a developed steady flow.

Reynolds stresses are neglected in the gas phase. No specific assumption is made on liquid Reynolds stresses.

Using the gas momentum balance equation, we can express analytically the void fraction profile as a function of the liquid velocity and pressure profiles.

From a physical viewpoint, our models are more appropriate for low Reynolds number ("laminar") bubbly flows. Nevertheless, because the derivation involves no assumption on liquid Reynolds stresses, our analytical solution can also be used as a verification tool for CFD simulations of high Reynolds number flows, provided the CFD code also neglects gas Reynolds stresses.

The analytical relation has two interests:

- Explaining with a simplified model the qualitative properties of void fraction profiles in pipes: void fraction peak near the wall for upward flows, void fraction maximum in the center of the pipe (core-peaking) for downward flows, cancellation of the void fraction at the wall.
- Verifying numerical codes, for instance assessing the grid refinement required near the wall.

We show that the void fraction profile results from an equilibrium between lift, wall and dispersion forces.

The effect of the lift force is seen to depend on the sign of the liquid velocity. If the lift coefficient is positive, upward flows push the bubbles towards the wall, whilst downward flows cause them to accumulate in the central region of the pipe, where the liquid velocity is (negative and) minimum. This behavior is illustrated by calculations with the NEPTUNE_CFD code.

In terms of grid resolution requirement, the comparison with our analytical solution emphasized the need for cells significantly smaller than the bubble size in order to correctly capture the void fraction peak near the wall.

Near the wall, the dominant effects are dispersion and wall forces, which counterbalance each other, and the void fraction tends to zero. It must be noted, however, that many models of dispersion force from the literature are derived in regions far away from the walls, where gradients (of velocity or velocity covariance) can be neglected. We believe the derivation of dispersion models specific to near-wall regions would be an important topic of investigation.

Acknowledgments

This work was performed in the frame of the NEPTUNE Project, financially supported by CEA (Commissariat à l'Energie Atomique), EDF (Electricité de France), IRSN (Institut de Radioprotection et de Sûreté Nucléaire) and AREVA-NP.

The authors would also like to thank the anonymous reviewers for their valuable suggestions which helped improve the manuscript.

References

Antal, S.P., Lahey Jr., R.T., Flaherty, J.E., 1991. Analysis of phase distribution in fully developed laminar bubbly two-phase flow. Int. J. Multiph. Flow 17 (5), 635–652.

Azpitarte, O.E., Buscaglia, G.C., 2003. Analytical and numerical evaluation of two-fluid model solutions for laminar fully developed bubbly two-phase flows. Chem. Eng. Sci. 58, 3765–3776.

Boyd, C., September 9–11 2014. Perspectives on CFD analysis in nuclear reactor regulation, Keynote Lecture, CFD4NRS-5 Conference, Zurich, Switzerland.

Burns, A.D.B., Grank, T. Hamill, I. Shi, J.M., 2004. The favre averaged drag model for turbulent dispersion in eulerian multi-phase flows. In: Proceedings of the 5th International Conference on Multiphase Flows ICMF, Yokohama, Japan.

Castillejos, A.H. Brimacombe, J.K., 1986. Structure of turbulent gas-liquid plumes in vertically injected jets. SCANINJECT IV, In: Proceedings of the Fourth International Conference on Injection Metallurgy, Lulea, Sweden, pp. 16:l–16:34.

Davidson, M.R., 1990. Numerical calculations of two-phase flow in a liquid bath with bottom gas injection: The central plume. Appl. Math. Modell. 14, 67–76.

Drew, D.A., Passman, S.L., 1999. Theory of Multicomponent Fluids. Springer, ISBN 0-387-98380-5.

Gosman, A.D., Lekakou, C., Politis, S., Issa, R.I., Looney, M.K., 1992. Multidimensional modeling of turbulent two-phase flows in stirred vessels. AIChE J. 38, 1946.

Guelfi, A., et al., 2007. NEPTUNE: a new software platform for advanced nuclear thermal hydraulics. Nucl. Sci. and Eng. 156, 281–324.

Guingo, M., et al., Recent Advances in Modeling and Validation of Nuclear Thermal-Hydraulics Applications with NEPTUNE_CFD, Proceedings of the ICAPP conference, Nice, 3-6 May 2015.

Ishii, M., Hibiki, T., 2010. Thermo-Fluid Dynamics of Two-Phase Flows. Springer http://dx.doi.org/10.1007/978-1-4419-7985-8.

Ishii, M., Kocamustafaogullari, G., 1983. Two-phase flow models and their limitations, S. Kakaç and M. Ishii (Eds.) Chap 1 of Advances in Two-Phase Flow and Heat Transfer, Fundamentals and Applications, Volume 1, Nato Science Series E, Springer.

Ishii, M., Zuber, N., 1979. Drag coefficient and relative velocity in bubbly, droplet or particulate flows. AIChE J. 25, 843–855.

Krepper, E. Lucas, D. Shi, J.M., Prasser, H.M., Simulations of FZR adiabatic air-water data with CFX-10, Nuresim European project, D.2.2.3.1.

Laviéville, J., Mérigoux, N. Guingo, M. Baudry, C., Mimouni, S., September 2015. A generalized turbulent dispersion model for bubbly flow numerical simulation in NEPTUNE_CFD. In: Proceedings of the NURETH-2015 conference, Chicago.

Liu, T.J., Bankoff, S.G., 1993. Structure of air-water bubbly flow in a vertical pipe – II. Void fraction, bubble velocity and bubble size distribution. Int. J. Heat Mass Transf. 36, 1061–1072.

Lopez de Bertodano, M., 1998. Two-fluid model for two-phase turbulent jet. Nucl. Eng. Des. 179 (11), 65–74.

Lopez de Bertodano, M.A., 1998. Two-fluid model for two-phase turbulent jets. Nucl. Eng. Des. 179, 65–74.

Morel, C., 2015. Mathematical Modeling of Disperse Two-Phase Flows. Springer http://dx.doi.org/10.1007/978-3-319-20104-7.

Podowski, M.Z., September 9–112014. Model verification and validation issues for multiphase flow and heat transfer simulation in reactor systems. Keynote Lecture, CFD4NRS-5 Conference, Zurich, Switzerland.

Pope, S.B., 2000. Turbulent flows. Cambridge University Press.

Tomiyama, A., June 1998. Struggle with computational bubble dynamics. In: Proceedings of the 3rd International Conference on Multiphase Flow ICMF 98, Lyon, France.

Wellek, R.M., Agrawal, A.K., Skelland, A.H.P., 1966. Shape of liquid drops moving in liquid media. AIChE J. 12, 854–862.